Organic Light-Emitting Diodes

Deutsche Ausgabe: DOI: 10.1002/ange.201506687
Internationale Ausgabe: DOI: 10.1002/anie.201506687

# Highly Efficient Near-Infrared Delayed Fluorescence Organic Light Emitting Diodes Using a Phenanthrene-Based Charge-Transfer Compound

*Shipan Wang, Xianju Yan, Zong Cheng, Hongyu Zhang, Yu Liu, and Yue Wang**

***Abstract:*** *Significant efforts have been made to develop high-efficiency organic light-emitting diodes (OLEDs) employing thermally activated delayed fluorescence (TADF) emitters with blue, green, yellow, and orange–red colors. However, efficient TADF materials with colors ranging from red, to deep-red, to near-infrared (NIR) have been rarely reported owing to the difficulty in molecular design. Herein, we report the first NIR TADF molecule TPA-DCPP (TPA = triphenylamine; DCPP = 2,3-dicyanopyrazino phenanthrene) which has a small singlet–triplet splitting ($\Delta E_{ST}$) of 0.13 eV. Its nondoped OLED device exhibits a maximum external quantum efficiency (EQE) of 2.1 % with a Commission International de L'Éclairage (CIE) coordinate of (0.70, 0.29). Moreover, an extremely high EQE of nearly 10 % with an emission band at $\lambda = 668$ nm has been achieved in the doped device, which is comparable to the most-efficient deep-red/NIR phosphorescent OLEDs with similar electroluminescent spectra.*

Thermally activated delayed fluorescence (TADF) materials have recently attracted great attention as a result of their promising applications in highly efficient fluorescent organic light-emitting diodes (OLEDs).[1–6] For efficient TADF molecules, a sufficiently small energy gap ($\Delta E_{ST}$) between the singlet ($S_1$) and triplet ($T_1$) states is desired to facilitate the reverse intersystem crossing (RISC) process. Theoretically, the $\Delta E_{ST}$ value can be minimized by controlling the separation of the highest occupied molecular orbital (HOMO) and the lowest unoccupied molecular orbital (LUMO) through molecular design.[1] Therefore, TADF is often observed in intramolecular-charge-transfer (ICT) systems containing spatially separated donor (D) and acceptor (A) moieties. Highly efficient TADF materials based on D–A chromophores with blue,[2] green,[3] yellow,[4] orange,[5] and red[6] colors have been studied and successfully utilized in fluorescent OLEDs (FOLEDs). However, it is still a challenge for researchers to develop efficient long-wavelength TADF emitters such as deep-red or near-infrared (NIR) TADF materials. The main reason for this is because simultaneously achieving a small $\Delta E_{ST}$ value and a large fluorescence rate ($k_F$) in one molecule is inherently difficult through molecular design. The limited orbital overlap required to obtain a small $\Delta E_{ST}$ value would generally lead to a low $k_F$ rate, which is detrimental to the obtainment of a high photoluminescence efficiency ($\Phi_{PL}$) for the system due to competition from radiationless transitions.[7] Furthermore, for deep-red/NIR emitters, the $\Phi_{PL}$ values tend to decrease as the emission wavelength increases, according to the energy-gap theory.[8] Additionally, many deep-red/NIR compounds exhibit weak or no emission in the solid state as a result of aggregation-caused quenching (ACQ).[9]

As a result of their potential applications in optical communication,[10] night-vision devices,[11] and sensors[12] deep-red/NIR OLEDs are attracting increasing interest.[13–16] To date, much effort has been made to develop NIR phosphorescent OLEDs (PHOLEDs) using osmium, iridium, or platinum metal–organic complexes.[13] However, high costs, limited resources of phosphorescent materials, and efficiency roll-offs at high current densities remain challenges for their application in long-term mass production. As an alternative material system, π-conjugated fluorophores with a D–A structure are raising particular interest for their tunable band-gap levels.[14a] However, for most NIR FOLEDs, low external quantum efficiencies (EQE < 1 %), resulting from a theoretical value of only 25 % of radiative excitons and a low fluorescence efficiency of D–A chromophores in the solid state, have become the bottleneck restricting their development.[14] Recently, Ma et al. reported an enhanced EQE of 1.54 % in a nondoped NIR FOLED employing a highly emissive D–A compound.[15] Nevertheless, there is still much room for improvement in NIR FOLEDs using metal-free highly luminescent organic materials.

TADF materials are ideal candidates to enhance efficiency in NIR FOLEDs. Herein, we report the first NIR TADF molecule TPA-DCPP, featuring a V-shaped D–π–A–π–D configuration with 2,3-dicyanopyrazino phenanthrene (DCPP) as the electron acceptor, diphenylamine (DPA) as the electron donor, and phenyl rings as π-conjugated bridges (Figure 1 a). We select a pyrazine derivative (DCPP) as the acceptor because of its large and rigid π-conjugated structure with a strong electron-withdrawing capability. DPA is used as the donor for its excellent hole-transporting capability and its steric hindrance that would diminish ACQ.[17] The DFT-optimized geometry of TPA-DCPP shows a relatively small dihedral angle of 35° between the DCPP-acceptor and the phenyl π-conjugated bridge (Figure 1 b). The small dihedral angle suggests a near-planar arrangement and thus moderate orbital overlaps can be anticipated. DFT calculations are performed on TPA-DCPP to study the molecular orbital distribution. The HOMO orbital is mainly distributed on the

[*] S. Wang, X. Yan, Z. Cheng, Prof. Dr. H. Zhang, Prof. Dr. Y. Liu, Prof. Dr. Y. Wang
State Key Lab of Supramolecular Structure and Materials
College of Chemistry, Jilin University
2699 Qianjin Avenue, Changchun, 130012 (P.R. China)
E-mail: yuewang@jlu.edu.cn

Supporting information for this article is available on the WWW under http://dx.doi.org/10.1002/anie.201506687.

  

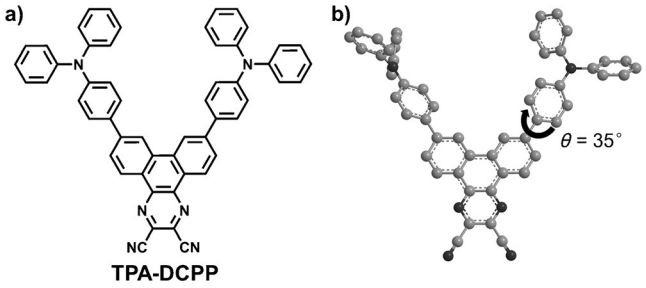


***Figure 1.*** a) Molecular structure of TPA-DCPP. b) DFT-optimized geometry of TPA-DCPP (B3LYP/6-31G(d,p) method).

DPA donor and the adjacent phenyl bridges, whereas the LUMO orbital is localized mainly on the DCPP acceptor and partly on the phenyl bridges (see Figure S1 in the Supporting Information). This molecular orbital distribution not only ensures an effective HOMO–LUMO separation, but also causes partial orbital overlaps which enhance the $k_F$ value. Additionally, a small $\Delta E_{ST}$ value can be anticipated in such an ICT systems with a relatively rigid structure containing spatially separated donor and acceptor moieties.[1a] As confirmed by time-dependent DFT (TD-DFT) calculations (Table S1), the theoretical $\Delta E_{ST}$ value of TPA-DCPP is estimated to be 0.20 eV. Thus, a small $\Delta E_{ST}$ and a large $k_F$ value can be simultaneously obtained by employing this molecular design.

TPA-DCPP was synthesized (Scheme S1) by a palladium-catalyzed Suzuki coupling reaction of the DCPP moiety with the triphenylamine (TPA) moiety. The thermal properties of TPA-DCPP were examined by differential scanning calorimetry (DSC) and thermogravimetric analysis (TGA; Figure S2). TPA-DCPP showed a high glass-transition temperature ($T_g$) of 165 °C and excellent thermal stability with a high decomposition temperature ($T_d$) of 508 °C, which was favorable to form uniform films upon thermal evaporation. The cyclic voltammogram of TPA-DCPP demonstrated reversible oxidation and reduction curves (Figure S3), indicating its good electrochemical stability. The HOMO and LUMO energy levels of TPA-DCPP were calculated to be −5.30 eV and −3.52 eV, respectively, which were obtained from the onsets of the oxidation and reduction curves.[18]

The UV/Vis absorption and photoluminescence (PL) spectra of TPA-DCPP in various solvents with different polarities are shown in Figure S4 and the photophysical data are summarized in Table 1 (for solutions of the compound in toluene and as a thin film). The lowest-energy absorption bands ($\lambda = 400$–$500$ nm) can be ascribed to the ICT transition originated from its D–π–A–π–D structure. TPA-DCPP displays a significant solvatochromic effect with remarkable red-shifts of the PL emission maxima from $\lambda = 504$ nm in the nonpolar solvent hexane to $\lambda = 810$ nm in the highly polar solvent dichloromethane ($CH_2Cl_2$). This large solvatochromic shift indicates a strong ICT state in TPA-DCPP, resulting in a large change in dipole moment in the excited state.[15] The phosphorescence spectrum at 77 K shows an emission band maximum at $\lambda = 600$ nm (Figure S5), different from that of DCPP or triphenylamine.[2a] The $\Delta E_{ST}$ value can be calculated from the onsets of the fluorescence and phosphorescence spectra,[5a] giving a $\Delta E_{ST}$ value as small as 0.13 eV. The $\Phi_{PL}$ values of TPA-DCPP in different solvents are summarized in Table S2. The highest $\Phi_{PL}$ value (84 %) was obtained in oxygen-free toluene. The transient PL decay for TPA-DCPP in oxygen-free toluene indicated the presence of only one component (monoexponential) with a lifetime ($\tau_F$) of 9.3 ns (Figure S6). Thus, a large $k_F$ value of $9.0 \times 10^{-7}$ $s^{-1}$ can be estimated from the $\Phi_{PL}$ and $\tau_F$ values. Unlike the behavior of conventional TADF molecules in fluid solution, its long-lived TADF emission may be completely quenched by nonradiative decay in solution, as revealed by some previously reported TADF compounds.[2a,b]

The photophysical properties of TPA-DCPP in the solid state were also studied. The pure TPA-DCPP thin film exhibited a broad NIR emission band with a maximum at $\lambda =$ 708 nm (Figure 2a; Table 1). Additionally, a remarkable $\Phi_{PL}$ value of 14 % was measured for the neat film. The transient PL decay of the TPA-DCPP film was biexponential, indicative of the presence of two components, in contrast to that recorded in solution (Figure 2b). A prompt fluorescence decay of 20.8 ns and a delayed fluorescence decay of 0.76 μs were observed in the time range of 2 μs. Furthermore, by doping TPA-DCPP in a host material of 1,3,5-tris(*N*-phenylbenzimidazol-2-yl)benzene (TPBi), a delayed emission with a much longer lifetime of 86.2 μs was also observed in a TPBi film doped with 10 wt % of TPA-DCPP (Figure 2c and Figure S7). In addition, the doped film showed a high $\Phi_{PL}$ value of 0.50 with an emission maximum of $\lambda = 645$ nm (Figure S8 and Table S3), suggesting an effective suppression of concentration quenching. To further confirm that the delayed fluorescence in the solid film originating from TADF, a temperature-dependent transient PL decay was conducted from 100 K to 300 K (Figure 2d). The ratio of the delayed component increased when the temperature was increased from 100 K to 300 K, demonstrating the presence of thermal activation energy for the TADF. Similar to the system reported by Adachi et al., the TADF emission of this molecule may occur through a mechanism that involves a reverse internal conversion (RIC) from the $^3\pi\pi^*$ state to the $^3$CT state, followed by RISC to the emissive $^1$CT state.[2a] In

***Table 1:*** Photophysical properties and thermal stability of TPA-DCPP.

| Compound | $\lambda_{abs}$ [nm] sol[a] | $\lambda_{em}$ [nm] sol[a]/film[b] | $\Phi_{PL}$ [%][c] sol[a]/film[b] | HOMO/LUMO [eV][d] | $E_S/E_T$ [eV][e] | $\Delta E_{ST}$ [eV][f] | $T_g/T_d$ [°C][g] |
|---|---|---|---|---|---|---|---|
| TPA-DCPP | 308, 368, 405, 458 | 588/708 | 84/14 | −5.30/−3.52 | 2.38/2.25 | 0.13 | 165/508 |

[a] Measured in oxygen-free toluene solution at room temperature ($10^{-5}$ M). [b] Measured in a neat film. [c] Absolute PL quantum yield evaluated using an integrating sphere. [d] Determined from cyclic voltammetry. [e] Singlet ($E_S$) and triplet ($E_T$) energies estimated from onsets of the fluorescence and phosphorescence spectra in toluene, respectively. [f] $\Delta E_{ST} = E_S - E_T$. [g] $T_d$ corresponds to 5 % weight loss temperature.

  

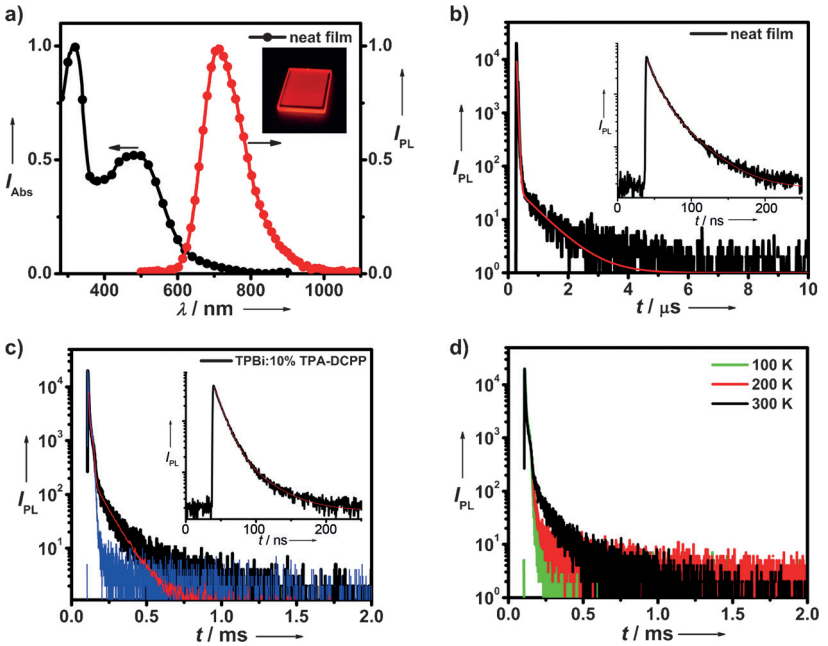


***Figure 2.*** a) The absorption (black) and PL (red) spectra of TPA-DCPP in a neat film. Inset: Image of the neat film under UV irradiation ($\lambda_{ex} = 365$ nm). b) Transient PL decay curves of TPA-DCPP in a neat film. Inset: Decay measured over a time range of 500 ns. c) Transient PL decay curves of a TPBi film doped with 10 wt%. Inset: Decay measured over a time range of 500 ns. Red curves are fitting data. Blue curves are instrument response factor (IRF) data. d) Temperature dependence of the transient PL spectra for the TPBi film doped with 10 wt% TPA-DCPP.

fluid solution, its low-lying $^3\pi\pi^*$ excitons tend to be easily deactivated by collisions with surrounding molecules.

Additionally, intramolecular vibration and rotation may be quite significant in such a twisted ICT molecule. Thus, the RIC process would be hindered and the TADF emission could not be observed in solution. DCPP is also known as a non-AIE (aggregation-induced emission) compound with "locked" phenyl rings.[19] In our case, TPA-DCPP is AIE-active. The PL spectra of TPA-DCPP in THF/water mixtures with different water fractions ($f_w$) are shown in Figure S9. Emission from the pure THF solution of TPA-DCPP is very weak. The PL intensity starts to increase abruptly when the $f_w$ value goes up to 70 vol% and is further enhanced by additional increases in the $f_w$ value. The enhancement of emission intensity is induced by the aggregation of molecules, thus suggesting that TPA-DCPP is AIE-active, similar to many previously reported twisted ICT molecules.[20]

As a result of the AIE–TADF properties of the molecule and its high thermal stability, we first fabricated a nondoped near-IR OLED device with the configuration of [ITO/NPB(80 nm)/TCTA(5 nm)/TPA-DCPP(20 nm)/TPBi(30 nm)/LiF-(0.5 nm)/Al], in which ITO is indium tin oxide, NPB is *N*,*N*′-bis(naphthalen-1-yl)-*N*,*N*′-bis(phenyl)benzidine, and TCTA is tris(4-carbazoyl-9-ylphenyl)amine. The energy diagram and chemical structures of the materials used in this device are shown in Figure S10. Despite the fact that our instrument (PR-650 Spectroscan spectrometer) could not detect the EL luminance signal over $\lambda = 780$ nm, the EL spectrum of the TPA-DCPP device was almost identical to the PL spectrum of the evaporated film (Figure 3a and Figure S11). The nondoped device exhibited NIR emission with an emission band maximum at $\lambda = 710$ nm and Commission Internationale de L'Éclairage (CIE) coordinates of (0.70, 0.29). A maximum EQE of 2.1% and brightness of 591 cd m$^{-2}$ were observed for the nondoped NIR OLED based on TPA-DCPP. The current-density–voltage–luminance (*J*–*V*–*L*) characteristics of the NIR OLED are shown in Figure 3b. The EQE of OLEDs is generally expressed by the following equation:

$$\mathrm{EQE} = (\gamma \times \eta_\gamma \times \Phi_{PL}) \times \eta_{out} \quad (1)$$

where $\eta_{out}$ is the light outcoupling efficiency (circa 20%), $\gamma$ is the recombination efficiency of injected holes and electrons (circa 100%), $\eta_\gamma$ is the efficiency of radiative exciton production, and $\Phi_{PL}$ is the quantum yield of the emitting layer (circa

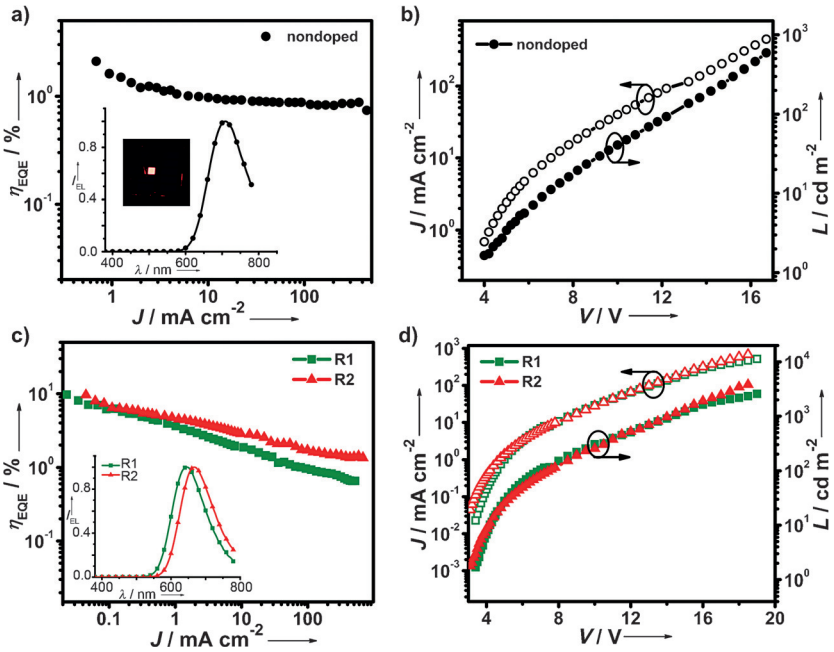


***Figure 3.*** a) EQE versus current density characteristics of the nondoped device. Inset: EL spectrum and image of the device at 5 V. b) The *J*–*V*–*L* characteristics of the nondoped device. c) EQE versus current density characteristics of the doped devices R1 and R2. Inset: EL spectra at 5 V. d) The *J*–*V*–*L* characteristics of the doped devices R1 and R2.

14%). Thus, a high $\eta_\gamma$ value of 75% is estimated for the nondoped device, far exceeding the 25% limit for radiative excitons in conventional FOLEDs, which is a result of thermally harvested triplet excitons. To our knowledge, the performance of the nondoped device is among the highest values (circa 2%) reported in nondoped NIR FOLEDs with similar EL spectra.[15]

We further fabricated two doped OLED devices with structures of [ITO/NPB(60 nm)/TCTA(5 nm)/EML(20 nm)/TPBi(30 nm)/LiF(0.5 nm)/Al], where EML, the emitting layer, is composed of TPBi doped with 10 wt% TPA-DCPP for device R1 and TPBi doped with 20 wt% TPA-DCPP for device R2, respectively. The EL spectra of these OLEDs are shown in the inset in Figure 3c, and are almost identical to the PL spectra of the doped films (Figure S8). The device R1 and R2 emit deep-red light with emission bands at $\lambda = 648$ nm and 668 nm and CIE coordinates of (0.64, 0.35) and (0.68, 0.32), respectively. Additionally, the EL spectra remain almost unchanged over a wide range of driving voltages, suggesting efficient energy transfer (Figure S12). The maximum EQEs of devices R1 and R2 are 9.6% and 9.8%, respectively, indicating that nearly 100% triplet harvesting is achieved in the doped devices considering the $\Phi_{PL}$ values of circa 0.50. Moreover, the high EQE value of R2 is even comparable to that of most efficient deep-red/NIR PHOLEDs (circa 14%) with similar spectra.[13b] The current-density–voltage–luminance (*J*–*V*–*L*) characteristics, current efficiencies (CE), and power efficiencies (PE) versus luminance curves of devices R1 and R2 are shown in Figure 3d and Figure S13. The device performances of the devices are summarized in Table S4. Device R2 shows a lower turn-on voltage of 3.1 V and a higher brightness of 3807 cd m$^{-2}$ compared with that of device R1 (3.4 V, 2577 cd m$^{-2}$). The maximum CE of device R1 and R2 are 7.4 cd A$^{-1}$ and 4.0 cd A$^{-1}$, respectively. Nevertheless, the devices exhibit a fast EQE roll-off with increasing current density. For example, the EQE of device R2 decreases to 3.0% and 1.5% at a luminance of 100 cd m$^{-2}$ and 1000 cd m$^{-2}$, respectively. This can be attributed to the long TADF lifetimes of TPA-DCPP in the doped film, which are more easily quenched by triplet–triplet annihilation (TTA) or singlet–triplet annihilation (STA) processes, as evidenced by previous studies.[6] We believe that the device performance will be further improved through optimized device structures with better host and transport materials.

In summary, a novel NIR TADF compound, TPA-DCPP, featuring a D–π–A–π–D structure has been designed and synthesized. Through careful molecular design, a small $\Delta E_{ST}$ value of 0.13 eV and a large $k_F$ value of $9.0 \times 10^{-7}$ s$^{-1}$ are simultaneously achieved in one molecule. TPA-DCPP exhibits a high $\Phi_{PL}$ value of 14% with an emission band maximum at $\lambda = 708$ nm in the neat film. The OLED device employing TPA-DCPP as a nondoped emitter exhibits a maximum EQE of 2.1% with CIE coordinates of (0.70, 0.29), which is among the highest values reported in nondoped NIR FOLEDs. Notably, the doped device achieves an extremely high EQE of 9.8% with an emission band maximum at $\lambda = 668$ nm, which is comparable to the values reported for most efficient deep-red/NIR PHOLEDs with similar EL spectra. Thus, TPA-DCPP is the first NIR TADF material applied to highly efficient deep-red/NIR OLEDs. We believe that our study provides a new method to design efficient organic NIR fluorescent molecules.

## Acknowledgements

This work was supported by the National Natural Science Foundation of China (91333201, 51173065, and 21221063) and the Program for Chang Jiang Scholars and Innovative Research Team in University (No. IRT101713018).

**Keywords:** charge transfer · delayed fluorescence · near-infrared luminescence · organic light-emitting diodes · photophysics

**How to cite:** *Angew. Chem. Int. Ed.* **2015**, *54*, 13068–13072
*Angew. Chem.* **2015**, *127*, 13260–13264

[1] a) H. Uoyama, K. Goushi, K. Shizu, H. Nomura, C. Adachi, *Nature* **2012**, *492*, 234–238; b) F. B. Dias, K. N. Bourdakos, V. Jankus, K. C. Moss, K. T. Kamtekar, V. Bhalla, J. Santos, M. R. Bryce, A. P. Monkman, *Adv. Mater.* **2013**, *25*, 3707–3714; c) S. Y. Lee, T. Yasuda, Y. S. Yang, Q. Zhang, C. Adachi, *Angew. Chem. Int. Ed.* **2014**, *53*, 6402–6406; *Angew. Chem.* **2014**, *126*, 6520–6524; d) Y. Tao, K. Yuan, T. Chen, P. Xu, H. Li, R. Chen, C. Zheng, L. Zhang, W. Huang, *Adv. Mater.* **2014**, *26*, 7931–7958.

[2] a) Q. Zhang, J. Li, K. Shizu, S. Huang, S. Hirata, H. Miyazaki, C. Adachi, *J. Am. Chem. Soc.* **2012**, *134*, 14706–14709; b) Q. Zhang, B. Li, S. Huang, H. Nomura, H. Tanaka, C. Adachi, *Nat. Photonics* **2014**, *8*, 326–332; c) M. Kim, S. K. Jeon, S.-H. Hwang, J. Y. Lee, *Adv. Mater.* **2015**, *27*, 2515–2520; d) Q. Zhang, D. Tsang, H. Kuwabara, Y. Hatae, B. Li, T. Takahashi, S. Y. Lee, T. Yasuda, C. Adachi, *Adv. Mater.* **2015**, *27*, 2096–2100; e) S. Hirata, Y. Sakai, K. Masui, H. Tanaka, S. Y. Lee, H. Nomura, N. Nakamura, M. Yasumatsu, H. Nakanotani, Q. Zhang, K. Shizu, H. Miyazaki, C. Adachi, *Nat. Mater.* **2015**, *14*, 330–336.

[3] a) H. Tanaka, K. Shizu, H. Miyazaki, C. Adachi, *Chem. Commun.* **2012**, *48*, 11392–11394; b) G. Méhes, H. Nomura, Q. Zhang, T. Nakagawa, C. Adachi, *Angew. Chem. Int. Ed.* **2012**, *51*, 11311–11315; *Angew. Chem.* **2012**, *124*, 11473–11477; c) Y. J. Cho, K. S. Yook, J. Y. Lee, *Adv. Mater.* **2014**, *26*, 6642–6646; d) Y. J. Cho, S. K. Jeon, B. D. Chin, E. Yu, J. Y. Lee, *Angew. Chem. Int. Ed.* **2015**, *54*, 5201–5204; *Angew. Chem.* **2015**, *127*, 5290–5293; e) C. Tang, T. Yang, X. Cao, Y. Tao, F. Wang, C. Zhong, Y. Qian, X. Zhang, W. Huang, *Adv. Opt. Mater.* **2015**, *3*, 786–790.

[4] a) T. Nakagawa, S. Y. Ku, K. T. Wong, C. Adachi, *Chem. Commun.* **2012**, *48*, 9580–9582; b) H. Wang, L. Xie, Q. Peng, L. Meng, Y. Wang, Y. Yi, P. Wang, *Adv. Mater.* **2014**, *26*, 5198–5204.

[5] a) J. Li, T. Nakagawa, Q. Zhang, H. Nomura, H. Miyazaki, C. Adachi, *Adv. Mater.* **2013**, *25*, 3319–3323; b) H. Tanaka, K. Shizu, H. Nakanotani, C. Adachi, *Chem. Mater.* **2013**, *25*, 3766–3771.

[6] Q. Zhang, H. Kuwabara, W. J. Potscavage, S. Huang, Y. Hatae, T. Shibata, C. Adachi, *J. Am. Chem. Soc.* **2014**, *136*, 18070–18081.

[7] a) A. P. Monkman, *ISRN Mater. Sci.* **2013**, 670130; b) D. D. Zhang, L. Duan, C. Li, Y. L. Li, H. Y. Li, D. Q. Zhang, Y. Qiu, *Adv. Mater.* **2014**, *26*, 5050–5055.

[8] a) J. V. Caspar, E. M. Kober, B. P. Sullivan, T. J. Meyer, *J. Am. Chem. Soc.* **1982**, *104*, 630–632; b) S. D. Cummings, R. Eisenberg, *J. Am. Chem. Soc.* **1996**, *118*, 1949–1960.

  

[9] a) A. C. Grimsdale, K. L. Chan, R. E. Martin, P. G. Jokisz, A. B. Holmes, *Chem. Rev.* **2009**, *109*, 897 – 1091; b) G. Qian, Z. Y. Wang, *Chem. Asian J.* **2010**, *5*, 1006 – 1029.

[10] a) N. Tessler, V. Medvedev, M. Kazes, S. Kan, U. Banin, *Science* **2002**, *295*, 1506 – 1508; b) B. Stender, S. F. Vçlker, C. Lambert, J. Pflaum, *Adv. Mater.* **2013**, *25*, 2943 – 2947.

[11] a) K. S. Schanze, J. R. Reynolds, J. M. Boncella, B. S. Harrison, T. J. Foley, M. Bouguettaya, T.-S. Kang, *Synth. Met.* **2003**, *137*, 1013 – 1014; b) D. Y. Kim, D. W. Song, N. Chopra, P. D. Somer, F. So, *Adv. Mater.* **2010**, *22*, 2260 – 2263.

[12] E. L. Williams, J. Li, G. E. Jabbour, *Appl. Phys. Lett.* **2006**, *89*, 083506.

[13] a) C. Borek, K. Hanson, P. I. Djurovich, M. E. Thompson, K. Aznavour, R. Bau, Y. R. Sun, S. R. Forrest, J. Brooks, L. Michalski, J. Brown, *Angew. Chem. Int. Ed.* **2007**, *46*, 1109 – 1112; *Angew. Chem.* **2007**, *119*, 1127 – 1130; b) M. Cocchi, J. Kalinowski, D. Virgili, J. A. G. Williams, *Appl. Phys. Lett.* **2008**, *92*, 113302; c) T.-C. Lee, J.-Y. Hung, Y. Chi, Y.-M. Cheng, G.-H. Lee, P.-T. Chou, C.-C. Chen, C.-H. Chang, C.-C. Wu, *Adv. Funct. Mater.* **2009**, *19*, 2639 – 2647; d) K. R. Graham, Y. Yang, J. R. Sommer, A. H. Shelton, K. S. Schanze, J. Xue, J. R. Reynolds, *Chem. Mater.* **2011**, *23*, 5305 – 5312; e) R. Tao, J. Qiao, G. Zhang, L. Duan, C. Chen, L. Wang, Y. Qiu, *J. Mater. Chem. C* **2013**, *1*, 6446 – 6454; f) T. Yu, D. P.-K. Tsang, V. K.-M. Au, W. H. Lam, M.-Y. Chan, V. W.-W. Yam, *Chem. Eur. J.* **2013**, *19*, 13418 – 13427; g) M. Schulze, A. Steffen, F. Würthner, *Angew. Chem. Int. Ed.* **2015**, *54*, 1570 – 1573; *Angew. Chem.* **2015**, *127*, 1590 – 1593; h) X. Cao, J. Miao, M. Zhu, C. Zhong, C. Yang, H. Wu, J. Qin, Y. Cao, *Chem. Mater.* **2015**, *27*, 96 – 104.

[14] a) G. Qian, B. Dai, M. Luo, D. Yu, J. Zhan, Z. Zhang, D. Ma, Z. Y. Wang, *Chem. Mater.* **2008**, *20*, 6208 – 6216; b) G. Qian, Z. Zhong, M. Luo, D. Yu, Z. Zhang, Z. Y. Wang, D. Ma, *Adv. Mater.* **2009**, *21*, 111 – 116; c) G. Qian, Z. Zhong, M. Luo, D. Yu, Z. Zhang, D. Ma, Z. Y. Wang, *J. Phys. Chem. C* **2009**, *113*, 1589 – 1595; d) X. Du, J. Qi, Z. Zhang, D. Ma, Z. Y. Wang, *Chem. Mater.* **2012**, *24*, 2178 – 2185; e) M. Shimizu, R. Kaki, Y. Takeda, T. Hiyama, N. Nagai, H. Yamagishi, H. Furutani, *Angew. Chem. Int. Ed.* **2012**, *51*, 4095 – 4099; *Angew. Chem.* **2012**, *124*, 4171 – 4175; f) Y. X. Yang, R. Farley, T. T. Steckler, S. H. Eom, J. R. Reynolds, K. S. Schanze, J. G. Xue, *Appl. Phys. Lett.* **2008**, *93*, 163305.

[15] L. Yao, S. T. Zhang, R. Wang, W. J. Li, F. Z. Shen, B. Yang, Y. G. Ma, *Angew. Chem. Int. Ed.* **2014**, *53*, 2119 – 2123; *Angew. Chem.* **2014**, *126*, 2151 – 2155.

[16] Q. Peng, A. Obolda, M. Zhang, F. Li, *Angew. Chem. Int. Ed.* **2015**, *54*, 7091 – 7095; *Angew. Chem.* **2015**, *127*, 7197 – 7201.

[17] S. Chen, X. Xu, Y. Liu, G. Yu, X. Sui, W. Qiu, Y. Ma, D. Zhu, *Adv. Funct. Mater.* **2005**, *15*, 1541 – 1546.

[18] C. M. Cardona, W. Li, A. E. Kaifer, D. Stockdale, G. C. Bazan, *Adv. Mater.* **2011**, *23*, 2367 – 2371.

[19] a) A. Qin, J. W. Y. Lam, F. Mahtab, C. K. W. Jim, L. Tang, J. Sun, H. H. Y. Sung, I. D. Williams, B. Z. Tang, *Appl. Phys. lett.* **2009**, *94*, 253308; b) C. Deng, Y. Niu, Q. Peng, A. Qin, Z. Shuai, B. Z. Tang, *J. Chem. Phys.* **2011**, *135*, 014304; c) Q. Wu, C. Deng, Q. Peng, Y. Niu, Z. Shuai, *J. Comput. Chem.* **2012**, *33*, 1862 – 1869.

[20] a) R. Hu, E. Lager, A. Aguilar-Aguilar, J. Liu, J. W. Y. Lam, H. H. Y. Sung, I. D. Williams, Y. Zhong, K. S. Wong, E. Pea-Cabrera, B. Z. Tang, *J. Phys. Chem. C* **2009**, *113*, 15845 – 15853; b) W. Z. Yuan, Y. Gong, S. Chen, X. Y. Shen, J. W. Y. Lam, P. Lu, Y. Lu, Z. Wang, R. Hu, N. Xie, H. S. Kwok, Y. Zhang, J. Z. Sun, B. Z. Tang, *Chem. Mater.* **2012**, *24*, 1518 – 1528; c) X. Y. Shen, W. Z. Yuan, Y. Liu, Q. Zhao, P. Lu, Y. Ma, I. D. Williams, A. Qin, J. Z. Sun, B. Z. Tang, *J. Phys. Chem. C* **2012**, *116*, 10541 – 10547; d) J. Zhang, B. Xu, J. Chen, L. Wang, W. Tian, *J. Phys. Chem. C* **2013**, *117*, 23117 – 23125; e) S. Xu, T. Liu, Y. Mu, Y. Wang, Z. Chi, C. Lo, S. Liu, Y. Zhang, A. Lien, J. Xu, *Angew. Chem. Int. Ed.* **2015**, *54*, 874 – 878; *Angew. Chem.* **2015**, *127*, 888 – 892.

Received: July 20, 2015
Published online: September 7, 2015

  